Experimental Study on the Combined Effect of Side Walls and Ambient Wind on the Height of Flame Ejected from the Opening of Fire Compartment

Fang X., Ren F., Zhang X.L., Sun X.P., Hu L.H.*

State Key Laboratory of Fire Science, University of Science and Technology of China, Hefei, Anhui, China
**Corresponding author's email: hlh@ustc.edu.cn*

ABSTRACT

This paper presents an experimental study on the flame height ejected from an opening of fire compartment over the façade constrained by two side walls under ambient wind. Experiments were carried out in a reduced-scale experimental model consisting of a cubic fire compartment with one opening and a façade wall. Two symmetrical side walls were set at the two sides of the opening along the façade, while the opening and the façade were set normal to ambient wind generated by a wind tunnel. The façade flame heights were measured by a CCD camera at various fuel supply rates or heat release rates, wind speeds and side wall separation distances. Results showed that the façade flame height decreased with increase in wind speed, while increased with decrease of side wall separation distance. Ambient wind was shown to affect the façade flame height relatively more significantly than the side walls. A scaling analysis was performed to interpret this behavior based on the air entrainment of the ejected flame under these conditions. Then a global non-dimensional factor K in relation to side wall separation distance, ambient wind speed, two characteristic length scales of the opening as well as the dimensionless excess heat release rate was brought forward to describe the façade flame height in various conditions. The experimental data are shown to be well correlated by the proposed function.

KEYWORDS: Compartment fire, façade flame, side wall, ambient wind.

NOMENCLATURE

A	area of opening (m^2)
$A\sqrt{H}$	ventilation factor ($m^{2.5}$)
C_p	specific heat of air at constant pressure (kJ/(kg·K))
D	side wall separation distance (m)
g	gravitational acceleration (9.8 m/s^2)
H	height of opening (m)
I	flame intermittency index
K	global non-dimensional correction factor
$\dot{m}_{front}$	air entrainment from front direction (kg/s)
$\dot{m}_{side}$	air entrainment from side direction (kg/s)
$\dot{Q}$	total heat release rate (kW)
$Z_{f(U_W,D)}$	façade flame height at an ambient wind of U_W and a side wall separation distance of D (m)

Greek

α	a coefficient characterizing the effect of ambient wind
$\tilde{\ell}$	characteristic air entrainment length scale (m)
ℓ_1	characteristic length scale of the opening, $\ell_1 = \left(A\sqrt{H}\right)^{2/5}$ (m)
ℓ_2	characteristic length scale of the opening, $\ell_2 = \left(AH^2\right)^{1/4}$ (m)

Proceedings of the Ninth International Seminar on Fire and Explosion Hazards (ISFEH9), pp. 672-683
Edited by Snegirev A., Liu N.A., Tamanini F., Bradley D., Molkov V., and Chaumeix N.
Published by St. Petersburg Polytechnic University Press
ISBN: 978-5-7422-6496-5 DOI: 10.18720/spbpu/2/k19-13

$\dot{Q}_{critical}$ critical heat release rate (kW)

$\dot{Q}_{ex}$ excess heat release rate (kW)

$\dot{Q}^*_{ex}$ dimensionless excess heat release rate

$\dot{Q}_{inside}$ heat release rate inside compartment (kW)

T_∞ ambient temperature (K)

U_W ambient wind speed (m/s)

W width of opening (m)

λ a coefficient describing the difference between front air entrainment and side air entrainment

ρ_∞ ambient air density (kg/m^3)

Subscripts

ex excess

∞ ambient conditions

f flame

Superscripts

* dimensionless

INTRODUCTION

Owing to the great threat to life and property, high-rise building façade fires have been a serious issue in current fire safety science research. In recent years, extensive research has been carried out to investigate the properties of façade flames ejected from an opening, including temperature profiles [1-5], façade flame heights [6-11], heat flux [7, 8, 12, 13] as well as the temperature inside the compartment [10, 14, 15].

As one of the most important ways of fire spreading to upper floors, façade flame height is one of the key parameters studied. For a free boundary condition, the façade flame ejected from a compartment fire can be physically regarded as generated by a rectangular fire source at the level of the neutral plane of the opening [7, 8], where the rectangular fire source has the side dimensions ℓ_1 ($\left(A\sqrt{H}\right)^{2/5}$, parallel to opening) and ℓ_2 ($\left(AH^2\right)^{1/4}$, normal to opening) with a heat release rate of $\dot{Q}_{ex}$. The façade flame height can be described as:

$$\frac{Z_{f(U_W=0,\,D=\infty)}}{\ell_1} = fcn\left(\dot{Q}^*_{ex}\right) = fcn\left(\frac{\dot{Q}_{ex}}{\rho_\infty C_p T_\infty \sqrt{g}\,\ell_1^{5/2}}\right), \tag{1}$$

where $Z_{f(U_W=0,D=\infty)}$ is the mean flame height (of 50% intermittency) above the neutral plane of the opening, ρ_∞ is ambient air density, C_p is specific heat of air at constant pressure, T_∞ is ambient air temperature, g is acceleration of gravity. $\dot{Q}^*_{ex}$ is the dimensionless excess heat release defined in terms of the excess heat release rate $\dot{Q}_{ex}$, which is the difference between the total heat release rate $\dot{Q}$ and the heat released inside the compartment for under-ventilated fires $\dot{Q}_{inside}$ [7, 8]:

$$\dot{Q}^*_{ex} = \frac{\dot{Q}_{ex}}{\rho_\infty C_p T_\infty \sqrt{g}\,\ell_1^{5/2}} = \frac{\dot{Q} - \dot{Q}_{inside}}{\rho_\infty C_p T_\infty \sqrt{g}\,\ell_1^{5/2}}\,. \tag{2}$$

However, the actual environment of high-rise building façade fires is usually complicated. In order to simulate the actual fire environment as much as possible, many researchers have also investigated some special experimental conditions. Lee et al. [16] studied the heat flux upon the façade due to ejected flame constrained by a front wall. Chen et al. [14] investigated the temperature inside the compartment under cross wind conditions with two dual openings on opposite walls. Hu et al. [9] studied the ejected flame behavior experimentally at two altitudes (ambient pressure effects).

For the case of the constraining effect on the façade fire due to side walls, results show that the façade flame is stretched to a high level and the flame height increases with decreasing side wall separation distance due to the reduction of the entrainment [10]. Conversely, for the case with ambient wind, the façade flame is depressed with its height decreasing as a result of the increment of the entrainment [17].

However, there is still no work studying how the façade flame behavior changes with the combined effect of side walls and ambient wind, which could exist simultaneously, despite the fact that these two cases are common factors in urban areas. Studying the combined effect of side wall and ambient wind on façade flame is also of importance to the fire community as these two factors have a completely different influence on the evolution of the façade flame height.

A series of experiments was carried out in the present work to study the ejected flame height over the façade with side walls under ambient wind. The combined effect of ambient wind and side walls on the façade flame was analyzed based on the change of air entrainment. A global non-dimensional factor K in relation to the wind speed, side wall separation distance and the characteristic length scales of the opening was proposed to describe the flame height in various conditions.

EXPERIMENTS

As shown in Fig. 1, a reduced-scale model consisting of a fire compartment with a vertical façade wall and two side walls is placed at the exit of a wind tunnel. The fire compartment is cubic with dimensions of 0.4 m and the inner wall is lined with 3 cm thick ceramic fiber board for thermal insulation [10, 11, 17]. The two side walls with dimensions of 0.6 m long and 1.3 m high are placed at each side of the compartment connecting to a façade wall of 1.5 m wide and 1.6 m high, both walls are made from a 5 mm thick fire resisting board (thermal conductivity is 0.085 W/(m·K)) and are supported by a steel structure. The separation distance between the two side walls is adjusted for different cases. The wind tunnel (20.2 m long with a square cross section of 1.8 m) [17] outlet exit is set to be normal to the opening and the façade. The provided ambient wind varies from 0 to 2 m/s at intervals of 0.5 m/s. The wind speed fluctuates less than 4% controlled by adjusting the rotating frequency of the fan. A four-probe anemometer with an accuracy of 0.01 m/s is placed at the exit of the wind tunnel to monitor the wind speed to ensure that it remains at the designated value.

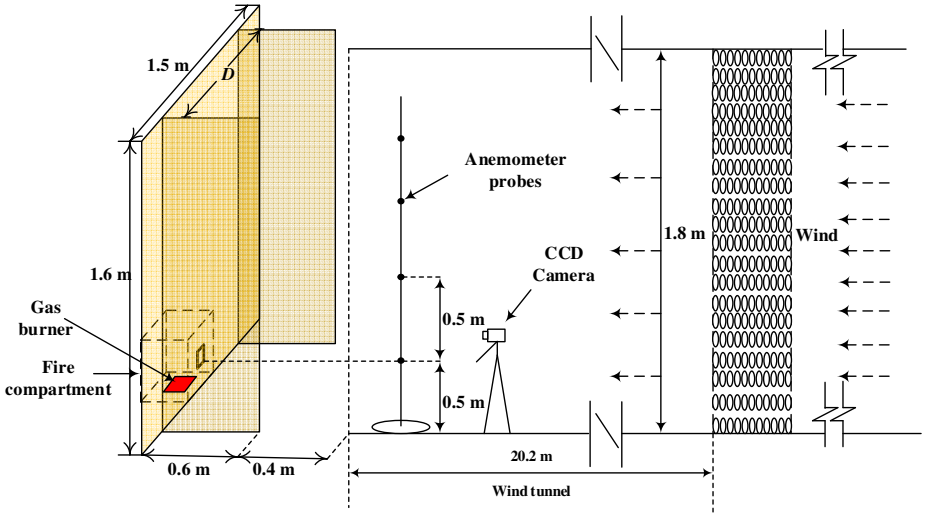

Fig. 1. Schematic of experimental setup.

Propane is used as fuel in the experiments and is fed to a square porous gas burner of 0.2 m with small holes of 0.5 cm diameter drilled on the upper surface at a spacing of 2 cm. The burner is placed at the center of the compartment floor with its upper surface flush with the floor. A gas fuel cylinder is connected to the burner through a flow meter with an accuracy of 0.01 SLPM (Standard Liter per Minute). The fuel supply rate is adjusted, and the total heat release rate is calculated through the mass flow rate and the fuel heat of combustion (50.4 MJ/kg) [10, 11, 17]. The experiments are controlled to be under-ventilated so that the flame ejects out of the opening.

Two different openings (dimensions 15 cm × 15 cm and 10 cm × 20 cm), representing two different ventilation factors ($A\sqrt{H}$), are employed in the experiment and installed at the center of the front surface of the compartment. All the experimental scenarios are summarized in Table 1, including opening dimensions, side wall separation distances, ambient wind speeds and total heat release rates. A total of 150 test cases are considered. The experiments are repeated three times for each case with the data fluctuation of mean flame height measured to be less than 3%. The averaged values are used for analysis and discussion.

Table 1. Summary of experimental scenarios

Test Series	Opening dimensions (m)	Side wall separation distance (m)	Wind speed (m/s)	*HRR* (kW)
1-75	0.15(W) × 0.15(H)	0.15, 0.30, 0.45, 0.6, ∞	0, 0.5, 1.0, 1.5, 2.0	37.0, 41.6, 46.2
76-150	0.10(W) × 0.20(H)			

A CCD camera (25 fps; sensor size 8.5 mm with 3,000,000 pixels) is used to record the ejected flame from the front view. For each case, the flame is recorded when the combustion condition reaches steady state after the total heat release rate remains at the set value for 8 min. Then a sampling time of 120 s (25 fps; 3000 consecutive snapshot images) of the ejected flame is recorded, and the distribution contour of flame appearance intermittency is obtained through image processing [18]. Finally, the mean flame height at intermittency I = 0.5 is obtained from the flame contour as typically shown in Fig. 2, which indicates a decrease of façade flame height with the increase of side wall separation distance and the increase of wind speed.

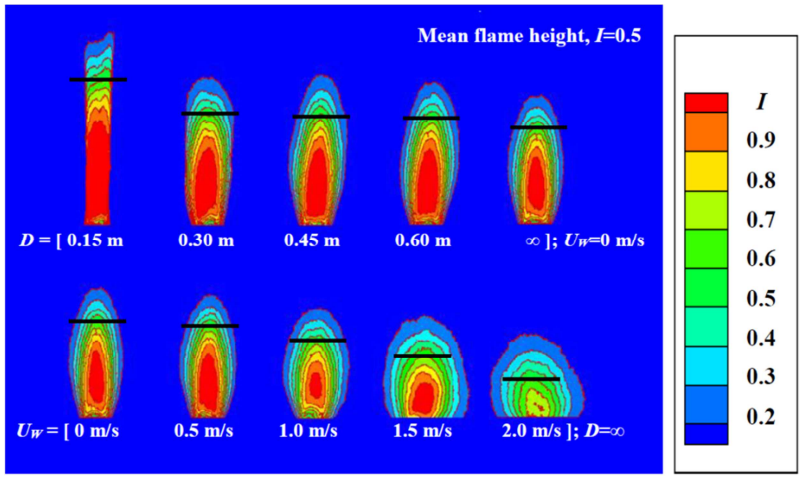

Fig. 2. Flame intermittency contour and determination of mean flame height (I = 0.5) without ambient wind and without side walls (opening: 15 cm × 15 cm is hidden; *HRR* = 41.6 kW).

RESULTS AND DISCUSSION

Mean flame height

Figure 3 shows the variation of flame height with ambient wind at various total heat release rates and side wall separation distances for the two openings. It is obvious that the flame height decreases with the increase in wind speed. Specifically, the flame height decreases significantly when the side wall separation distance increases from 0.15 to 0.30 m, while decreases much more slightly when the side wall separation distance increases from 0.30 m to ∞ (no side walls). The results for the façade flame height are similar to those in [10, 17] to a certain extent. However, the combined effect of side walls and ambient wind on the ejected flame remains to be quantified.

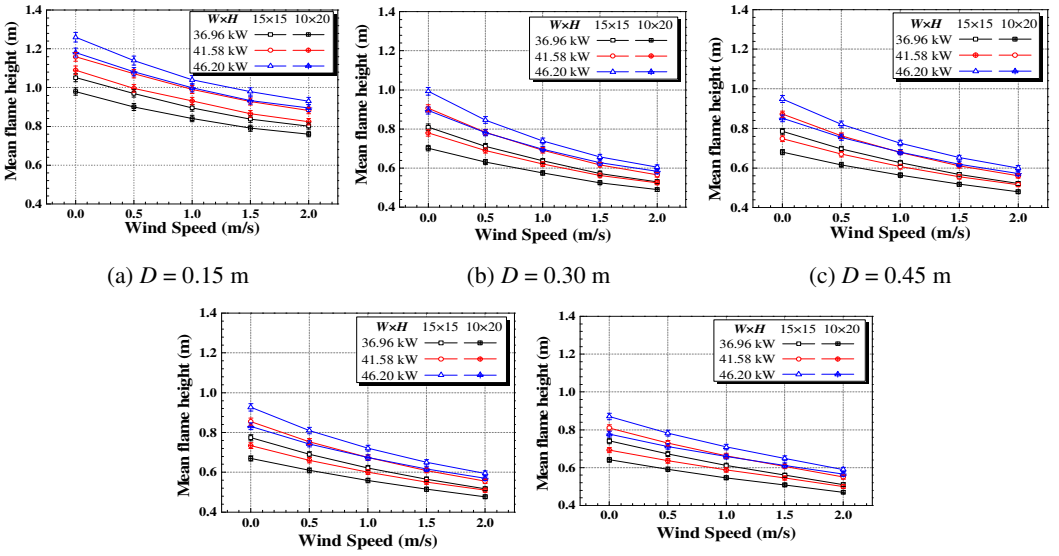

(a) D = 0.15 m (b) D = 0.30 m (c) D = 0.45 m

(d) D = 0.60 m (e) D = ∞

Fig. 3. Measured flame height at various total heat release rate under two openings for various side wall separation distances.

Combined effect of side walls and ambient wind on façade flame and mechanism analysis

In order to illustrate the effect of side walls on the ejected flame, $Z_{f(U_W=u,D)}/Z_{f(U_W=u,D=\infty)}$ is calculated referring to the ratio of flame height for a given ambient wind speed with side walls to that without side walls (the other parameters (opening dimensions, total heat release rate $\dot{Q}$ and wind speed U_W) remain unchanged). The evolution of the ratio $Z_{f(U_W=u,D)}/Z_{f(U_W=u,D=\infty)}$ with the side wall separation distance is shown in Fig. 4. The ratio is shown to decrease with increasing side wall separation distance. That is to say, the presence of side walls promotes the development of the ejected flame in ambient wind conditions, and the promotion effect increases gradually as the side wall separation distance decreases (side wall separation distance is greater than ℓ_1 where entrainment is constrained for an "axisymmetric fire" when $\dot{Q}^*_{ex}$ > 1.3 [10, 11]).

It is also not difficult to find an antagonistic effect between ambient wind and side walls. Specifically, side walls reduce the depression effect of ambient wind on the façade flame, and ambient wind reduces the promotion effect of the side walls on the façade flame as well. In addition, the façade flame height increases slowly with the decrease of side wall separation distance while it

decreases rapidly with the increase of wind speed. In other words, the promotion effect of side walls on the ejected flame shows to be much weaker than the depression effect of ambient wind.

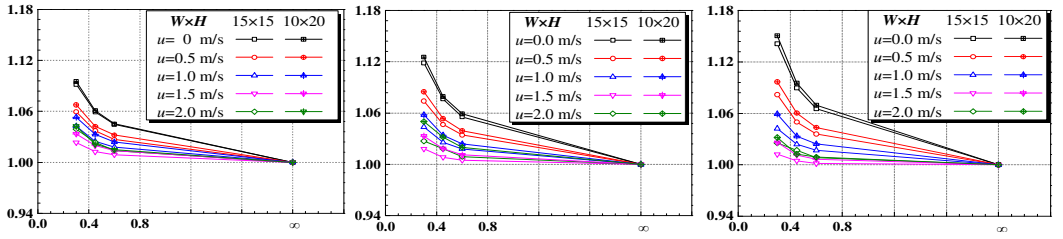

(a) HRR= 37.0 kW (b) HRR= 41.6 kW (c) HRR= 46.2 kW

Fig. 4. Variations of $Z_{f(U_W=u,D)}/Z_{f(U_W=u,D=\infty)}$ with side wall separation distance, D (m).

The same method is employed to illustrate the effect of ambient wind on the ejected flame. $Z_{f(U_W,D=d)}/Z_{f(U_W=0,D=d)}$ refers to the ratio of flame height for a given side wall separation distance with ambient wind to that without ambient wind. The evolution of the ratio $Z_{f(U_W,D=d)}/Z_{f(U_W=0,D=d)}$ against the wind speed is shown in Fig. 5. The ratio shows a significant decrease with the increase of wind speed, indicating that the ambient wind depresses the ejected flame constrained by the side walls and the depression effect increases as the wind speed increases.

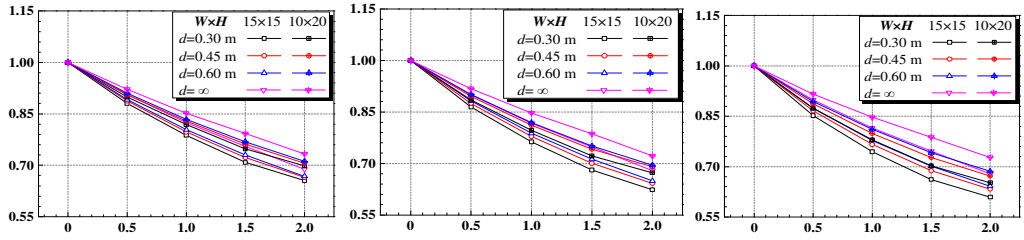

(a) HRR= 37.0 kW (b) HRR= 41.6 kW (c) HRR= 46.2 kW

Fig. 5. Variations of $Z_{f(U_W,D=d)}/Z_{f(U_W=0,D=d)}$ with ambient wind speed, U_W(m/s).

Essentially, the façade flame behavior originates from the combustion of the excess fuel ejected out of the opening [7, 8, 10, 17] involving the excess heat release rate $\dot{Q}_{ex}$, which is equal to the total heat release rate minus the heat release rate inside the compartment for under-ventilated fires as expressed in Eq. (2). Based on the fact that the temperature inside the compartment remains stable after the flame is ejected [10, 19], an assumption was made that $\dot{Q}_{inside}$ equals the critical heat release rate ($\dot{Q}_{critical}$) when the flame begins to come out of the opening:

$$\dot{Q}_{inside} = \dot{Q}_{critical} . \tag{3}$$

$\dot{Q}_{critical}$ was measured experimentally by increasing the *HRR* until flame ejection began under different wind speeds and side wall separation distances for the two openings. Thus, the value of $\dot{Q}_{ex}$ can be expressed as:

$$\dot{Q}_{ex} = \dot{Q} - \dot{Q}_{critical} \cdot \tag{4}$$

Figure 6 shows the values of $\dot{Q}_{critical}$ measured in the experiments against the wind speed for various side wall separation distances and opening sizes. It is shown that the presence of side walls hardly affects the critical heat release rate, which is consistent with the observation in [10, 11]. This result can be attributed to the air supply through the opening into the compartment mainly coming from the front direction. However, the critical heat release rate first increases and then decreases with the increase of wind speed, which is consistent with the results in [17, 19]. This can be interpreted as being due to the lower speed wind flow enhancing the entry of air into the compartment and promoting combustion inside, while higher speed wind flows ejects some of the fuel out of the compartment and depresses combustion inside [17]. As a comparison, the effect of ambient wind on the façade flame is reflected not only in the change of façade flame shape, but also in the influence of the excess heat release rate which is different from that due to the side walls.

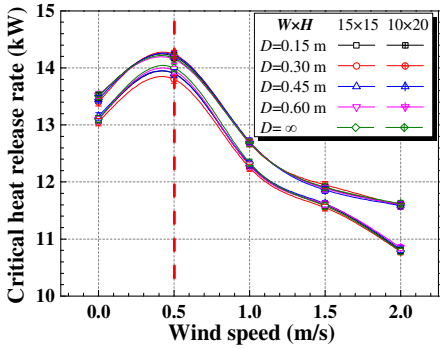

Fig. 6. Variation of the critical heat release rate with side wall separation distance and wind speed.

The mechanism of the combined effect of side walls and ambient wind on the façade flame is now analyzed based on air entrainment. For free boundary cases as shown in Fig. 7(a), the characteristic air entrainment length of the ejected flame is quantified as $\ell_1 + 2\lambda\ell_2$, in which ℓ_1 and $2\lambda\ell_2$ represent the front and side entrainment, respectively and $\lambda = 0.317\dot{Q}_{ex}^{*\,2/5} - 0.352$ describes the difference between them [10]. While the ejected flame is constrained by the side walls at a distance D ($> \ell_1$), front entrainment is not affected. Side entrainment is depressed with characteristic air entrainment length scales of ℓ_1 and $2\lambda\ell_2\left(1-\ell_1/D\right)$, respectively as shown in Fig. 7(b) [10]. For the cases of ambient wind condition, front entrainment is promoted while side entrainment is depressed with characteristic air entrainment length scales turning into $\ell_1\left(1+\alpha U_W/\sqrt{gH}\right)$ and $2\lambda\ell_2\left(1-\alpha U_W/\sqrt{gH}\right)$ (where $\alpha = 0.8\dot{Q}_{ex}^{*\,2/5} - 0.76$ is a linear coefficient characterizing the impact of ambient wind [17]), respectively as shown in Fig. 7(c) [17].

In summary, the side walls affect the side air entrainment while ambient wind affects both the front and the side air entrainment [10, 11, 17]. After noting that $\dot{Q}_{critical}$ varies with ambient wind speed while changes little with side wall separation distance as shown in Fig. 6, an assumption can be made that the side walls still only affect the side air entrainment while ambient wind affects both (side and front entrainment) when side walls and ambient wind are simultaneously present. An air entrainment model is then proposed as shown in Fig. 7(d), in which the characteristic air entrainment length scale from the front direction is $\ell_1\left(1+\alpha U_W/\sqrt{gH}\right)$, and the characteristic air

entrainment length scale from the side direction is $2\lambda\ell_2\left(1-\ell_1/D\right)\left(1-\alpha U_W/\sqrt{gH}\right)^{\exp(-\ell_1/D)}$. Obviously, the new proposed model is still applicable to the cases where the side walls or the ambient wind are present alone.

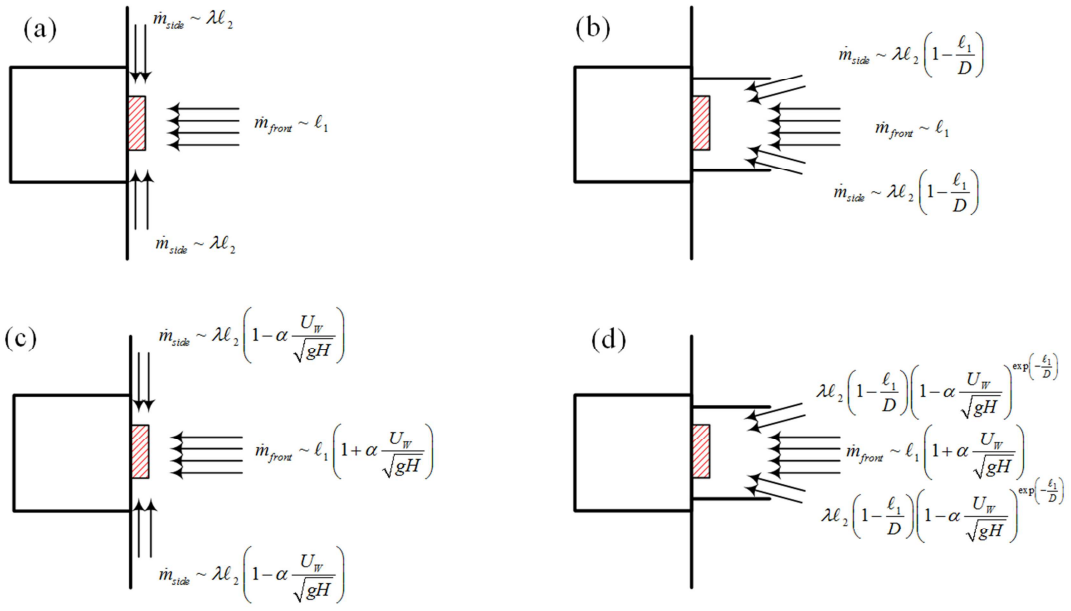

Fig. 7. Entrainment model of ejected flame for various conditions.

The combined effect of side walls and ambient wind on the façade flame mentioned above (shown in Fig. 4 and Fig. 5) is tentatively explained based on the proposed model. Since the air entrainment flow is proportional to the characteristic air entrainment length scale [10, 11, 17], the ratio of the side to the front air entrainment, $\dot{m}_{side}/\dot{m}_{front}$, is calculated through the following expression:

$$\frac{\dot{m}_{side}}{\dot{m}_{front}} = 2\lambda\ell_2\left(1-\frac{\ell_1}{D}\right)\left(1-\alpha\frac{U_W}{\sqrt{gH}}\right)^{\exp\left(-\frac{\ell_1}{D}\right)}\left(\ell_1\left(1+\alpha\frac{U_W}{\sqrt{gH}}\right)\right)^{-1}. \tag{5}$$

Noting that $\lambda = 0.317\dot{Q}_{ex}^{*\,2/5} - 0.352$ and $\alpha = 0.8\dot{Q}_{ex}^{*\,2/5} - 0.76$, $\dot{m}_{side}/\dot{m}_{front}$ can be expressed as a function of $\dot{Q}_{ex}^{*}$, D, U_W as a simplification. For the cases of a free boundary condition with no wind or side walls, the ratio of the side to the front air entrainment is $2\lambda\ell_2/\ell_1$ which increases with the increase of $\dot{Q}_{ex}^{*}$. The value of $\dot{Q}_{ex}^{*}$ is usually relatively low in the experiments and thus $\dot{m}_{side}/\dot{m}_{front}$ is much less than 1 indicating that front air entrainment is much stronger than side air entrainment [10, 11, 17]. This conclusion can be extended to cases with side walls or ambient wind through the calculation of the characteristic air entrainment length scale. Then a basic conclusion is reached that the front air entrainment plays a major role.

Figure 8 shows the variation of calculated $\dot{m}_{side}/\dot{m}_{front}$ with side wall separation distance for different total heat release rates and opening sizes. $\dot{Q}_{ex}^{*}$ varies little with side wall separation distance indicating that values of λ and α remain nearly unchanged. According to the air entrainment

model proposed above, it can be seen that with the increase of the side wall separation distance, the front air entrainment ($\sim \ell_1\left(1+\alpha U_W/\sqrt{gH}\right)$) remains unchanged while the side air entrainment ($\sim 2\lambda\ell_2\left(1-\ell_1/D\right)\left(1-\alpha U_W/\sqrt{gH}\right)^{\exp(-\ell_1/D)}$) increases gradually and so $\dot{m}_{side}/\dot{m}_{front}$ increases gradually. Meanwhile, the flame height is inversely proportional to the total entrainment [10, 17], which explains the phenomenon in Fig. 4, where the $Z_{f(U_W=u,D)}/Z_{f(U_W=u,D=d)} \sim D$ curve shows a decrease with increasing D. As the decreasing trend is seen to be relatively slow, it could be attributed to the fact that the front air entrainment is much stronger than that from the side direction, as previously recognized, and is not affected by side walls.

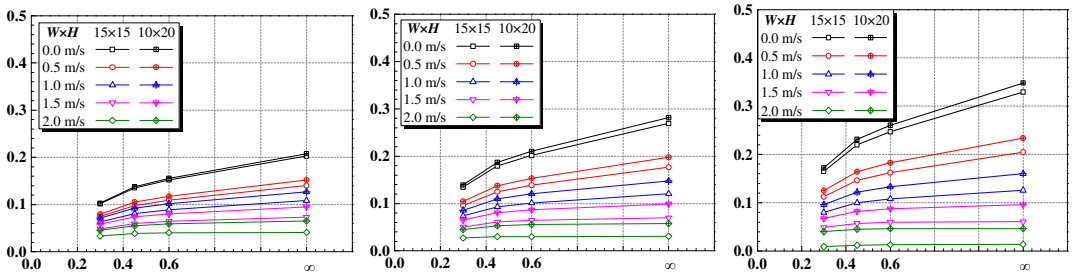

(a) HRR= 37.0 kW (b) HRR= 41.6 kW (c) HRR= 46.2 kW

Fig. 8. Variations of $\dot{m}_{side}/\dot{m}_{front}$ with side wall separation distance, D (m).

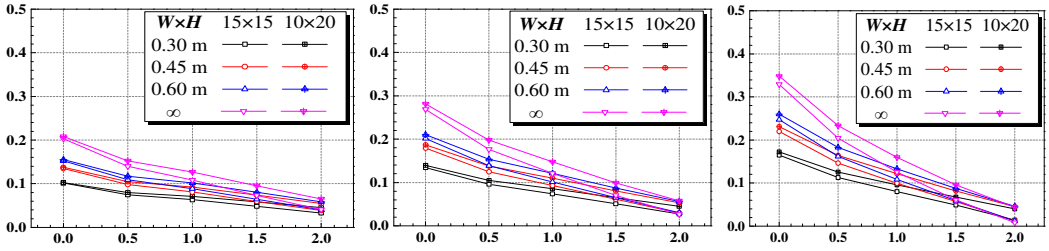

(a) HRR= 37.0 kW (b) HRR= 41.6 kW (c) HRR= 46.2 kW

Fig. 9. Variations of $\dot{m}_{side}/\dot{m}_{front}$ with ambient wind speed, U_W (m/s).

Figure 9 shows the variation of calculated $\dot{m}_{side}/\dot{m}_{front}$ with wind speed. As shown in Fig. 7(d), ambient wind promotes front air entrainment while depresses side air entrainment, thus $\dot{m}_{side}/\dot{m}_{front}$ decreases with the increase of wind speed. Although ambient wind affects the $\dot{Q}^*_{ex}$ thus changing the values of λ and α a little, analysis shows that it does not affect the trends of variations of side ($\sim 2\lambda\ell_2\left(1-\ell_1/D\right)\left(1-\alpha U_W/\sqrt{gH}\right)^{\exp(-\ell_1/D)}$) and front entrainment ($\sim \ell_1\left(1+\alpha U_W/\sqrt{gH}\right)$) with wind speed as the total heat release rate rises to a certain extent. And the total air entrainment increases with wind speed due to the much greater importance of the front air entrainment which controls mainly the total air entrainment. So, the flame height drops rapidly with wind speed, and the $Z_{f(U_W,D=d)}/Z_{f(U_W=0,D=d)} \sim U_W$ curve in Fig. 5 shows a significantly decrease with the increase of U_W as a result. This is also the main reason why the depression effect of ambient wind on the ejected

flame is much stronger than the promotion effect of side walls which does not affect front air entrainment.

Correction of flame height under the combined effect of side walls and ambient wind

An air entrainment model under the combined effect of side walls and ambient wind has been established, providing a good description of the variation of flame height with side wall separation distance and wind speed. The proposed air entrainment model will now be used as the basis for development of a quantitative prediction model of façade flame height.

As illustrated by Fig. 7(d), the characteristic air entrainment length scale constrained by side walls under ambient wind is $\tilde{\ell} = \ell_1\left(1+\alpha U_W/\sqrt{gH}\right)+2\lambda\ell_2\left(1-\ell_1/D\right)\left(1-\alpha U_W/\sqrt{gH}\right)^{\exp(-\ell_1/D)}$. It is usually recognized that air entrainment varies proportionally to a characteristic air entrainment length scale and the fact that flame height varies inversely with air entrainment [10, 17]. Based on the characteristic air entrainment length scale $\tilde{\ell} = \ell_1 + 2\lambda\ell_2$ for free boundary cases, a non-dimensional correction factor K is proposed to describe the façade flame height constrained by side walls under ambient wind:

$$K = \frac{Z_{f(U_W,D)}}{Z_{f(U_W=0,D=\infty)}} = \left(\ell_1 + 2\lambda\ell_2\right)\left(\ell_1\left(1+\alpha\frac{U_W}{\sqrt{gH}}\right)+2\lambda\ell_2\left(1-\frac{\ell_1}{D}\right)\left(1-\alpha\frac{U_W}{\sqrt{gH}}\right)^{\exp\left(-\frac{\ell_1}{D}\right)}\right)^{-1}, \tag{6}$$

which agrees with the expressions in [10, 17] and applies to cases where side walls or ambient wind exist alone. The detailed expression for K is:

$$K = \frac{Z_{f(U_W,D)}}{Z_{f(U_W=0,D=\infty)}} = \tag{7}$$

$$\frac{\ell_1 + 2\left(0.317\dot{Q}_{ex}^{*\,2/5} - 0.352\right)\ell_2}{\ell_1\left[1+\left(0.8\dot{Q}_{ex}^{*\,2/5} - 0.76\right)\frac{U_W}{\sqrt{gH}}\right]+2\left(0.317\dot{Q}_{ex}^{*\,2/5} - 0.352\right)\ell_2\left(1-\frac{\ell_1}{D}\right)\left[1-\left(0.8\dot{Q}_{ex}^{*\,2/5} - 0.76\right)\frac{U_W}{\sqrt{gH}}\right]^{\exp\left(-\frac{\ell_1}{D}\right)}}$$

Then the façade flame heights constrained by side walls with ambient wind corrected by the proposed factor K, $Z_{f(U_W,D)}/K$, versus those without side walls or ambient wind, $Z_{f(U_W=0,D=\infty)}$ are plotted in Fig. 10. The values are almost entirely distributed over the line $y = x$, indicating that K is appropriate for correcting the flame height under the combined effect of side walls and ambient wind.

CONCLUSIONS

The flame height ejected from an opening of a fire compartment over the façade constrained by side walls under ambient wind was studied in this paper. The combined effect of side walls and ambient wind on the façade flame height was revealed and quantified based on the analysis of the air entrainment and the excess heat release rate. Finally, a new correction global factor K was proposed to correlate the flame height. The main conclusions include:

1) There is a competition between the ambient wind and side walls for façade flame height. Side walls reduce the depression effect of ambient wind on the façade flame, while ambient wind reduces the promotion effect of the side walls on the façade flame, even when these two factors are both present. Ambient wind affects the flame height more significantly in comparison with side walls. As an estimate, side walls increase the flame height generally by less than 10%.

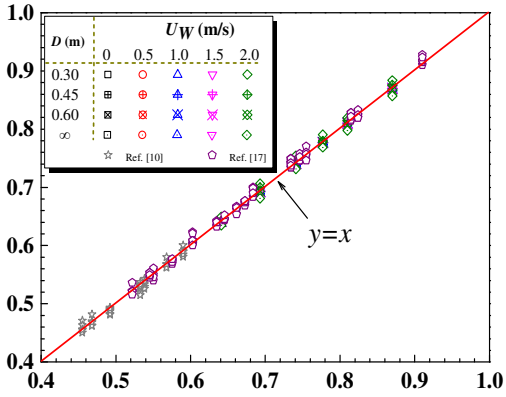

Fig. 10. Corrected flame heights $Z_{f(U_W,D)}/K$ versus those without side walls or ambient wind $Z_{f(U_W=0,D=0)}$.

2) The effect of ambient wind on the façade flame of a compartment fire is reflected in the two aspects of changing the ventilation of the fire compartment through the opening and affecting the air entrainment of the façade flame. On the other hand, the presence of side walls only results in the depression of air entrainment.

3) A new non-dimensional global factor is proposed to correlate the façade flame height based on the scaling analysis of the air entrainment in relation to ambient wind speed, side wall separation distance, the two characteristic length scales of the opening as well as the dimensionless excess heat release rate.

ACKNOWLEDGMENTS

This paper was supported by the Key project of National Natural Science Foundation of China (NSFC) under Grant No. 51636008, NSFC-STINT joint international exchange project (51811530015), Key Research Program of Frontier Sciences of Chinese Academy of Science (CAS) under Grant No. QYZDB-SSW-JSC029 and Fundamental Research Funds for the Central Universities under Grant no. WK2320000035 and WK2320000038.

REFERENCES

[1] S. Yokoi, Study on the Prevention of Fire Spread Caused by Hot Upward Current, Report No. 34, BRI, 1960.

[2] L. Seigel, The projection of flames from burning buildings, Fire Technol. 5 (1969) 43-51.

[3] J. Yamaguchi, T. Tanaka, Temperature Profiles of Window Jet Plume, In: Curtat, M. (Ed.), Fire Safety Science–Proceedings of the Sixth International Symposium, pp, 1a-3, 2004.

[4] K. Himoto, T. Tsuchihashi, Y. Tanaka, T. Tanaka, Modeling thermal behaviors of window flame ejected from a fire compartment, Fire Saf. J. 44.2 (2009) 230-240.

[5] Y. Ohmiya, Y. Hori, K. Safimori, T. Wakamatsu, Predictive method for properties of flame ejected from an opening incorporating excess fuel, In: Kashiwagi, T. (Ed.), Fire Safety Science–Proceedings of the Fourth International Symposium, pp, 375-386, 2000.

[6] M. Coutin, J.M. Most, M.A. Delichatsios, M.M. Delichatsios, Flame heights in wall fires: effects of width, confinement and pyrolysis length, In: Curtat, M. (Ed.), Fire Safety Science–Proceedings of the Sixth International Symposium, pp, 729-740, 2000.

[7] Y.P. Lee, M.A. Delichatsios, G.W.H. Silcock, Heat fluxes and flame heights in façades from fires in enclosures of varying geometry, Proc. Combust. Inst. 31 (2007) 2521–2528.

[8] Y.P. Lee, Heat fluxes and flame heights in external façade fires, PhD thesis, University of Ulster, Jordanstown, Northern Ireland, 2006.

[9] L.H. Hu, F. Tang, M.A. Delichatsios, Q. Wang, K.H. Lu, X.C. Zhang, Global behaviors of enclosure fire and façade flame heights in normal and reduced atmospheric pressures at two altitudes, Int. J. Heat. Mass Transf. 56 (2013) 119-126.

[10] L.H. Hu, K.H. Lu, F. Tang, M.A. Delichatsios, L.H. He, A global non-dimensional factor characterizing side wall constraint effect on façade flame entrainment and flame height from opening of compartment fires, Int. J. Heat. Mass Transf. 75 (2014) 122–129.

[11] K.H. Lu, L. H. Hu, F. Tang, L.H. He, X.C. Zhang, Z.W. Qiu, Experimental investigation on window ejected façade flame heights with different constraint side wall lengths and global correlation, Int. J. Heat. Mass Transf. 78 (2014) 17-24.

[12] F. Tang, L.H. Hu, Z. W. Qiu, X.C. Zhang, K.H. Lu, Window ejected flame height and heat flux along façade with air entrainment constraint by a sloping facing wall, Fire Saf. J. 71 (2015) 248-256.

[13] I. Oleszkiewicz, Fire exposure to exterior walls and flame spread on combustible cladding, Fire Technol. 26 (1990) 357-375.

[14] H. Chen, N. Liu, W. Chow, Wind effects on smoke motion and temperature of ventilation-controlled fire in a two-vent compartment, Build. Environ. 44 (2009) 2521-2526.

[15] F. Tang, L.H. Hu, M.A. Delichatsios, K.H. Lu, W. Zhu, Experimental study on flame height and temperature profile of buoyant window spill plume from an under-ventilated compartment fire, Int. J. Heat. Mass Transf. 55 (2012) 93-101.

[16] Y.P. Lee, M.A. Delichatsios, Y. Ohmiya, K. Wakatsuki, A. Yanagisawa, D. Goto, Heat fluxes on opposite building wall by flames emerging from an enclosure, Proc. Combust. Inst. 32 (2009) 2551-2558.

[17] L.H. Hu, K.Z. Hu, F. Ren, X.P. Sun, Façade flame height ejected from an opening of fire compartment under external wind, Fire Saf. J. 92 (2017) 151–158.

[18] N. Otsu, A threshold selection method from gray-level histograms, IEEE Trans. Syst. Man. Cybern. 9 (1979) 62-66.

[19] L. Hu, F. Ren, K. Hu, F. Tang, K. Lu, An experimental study on temperature evolution inside compartment with fire growth and flame ejection through an opening under external wind, Proc. Combust. Inst. 36 (2017) 2955-2962.